

# EFFECT OF POLY (N- VINYPYRROLIDONE) ON THE NON-ISOTHERMAL CRYSTALLIZATION KINETICS AND VISCOELASTIC PROPERTIES OF PVDF FILMS

A. Mashak<sup>1\*</sup>, A. Ghaee<sup>2</sup> and F. Ravari<sup>3</sup>

<sup>1</sup>Department of Novel Drug Delivery Systems, Iran Polymer and Petrochemical Institute, P.O. Box: 14965/115, Tehran, Iran.

\*E-mail: a.mashak@ippi.ac.ir

<sup>2</sup>Department of Life Science Engineering, Faculty of New Sciences and Technologies, University of Tehran, P.O. Box: 143951374, Tehran, Iran.

<sup>3</sup>Department of Chemistry, Payame Noor University, Tehran 19395-4697, Iran.

(Submitted: March 15, 2015 ; Revised: August 24, 2015 ; Accepted: August 28, 2015)

**Abstract** - Poly(vinylidene fluoride) (PVDF) and PVDF blends with various molecular weights of poly (N-vinylpyrrolidone) (PVP) films were prepared in dimethyl formamide through the solution casting method. Non-isothermal melt crystallization studies of PVDF films were carried out by cooling the molten samples at different temperatures using differential scanning calorimetry (DSC). The obtained films have been characterized by dynamic mechanical thermal analysis (DMTA). Crystallization kinetics of PVDF films were successfully described by the Jeziorny, Mo and Ziabicki models. The Ozawa equation was found to be invalid for describing the crystallization kinetics. Kinetic parameters such as  $t_{1/2}$ ,  $Z_c$  and  $F(T)$  indicated that the crystallization rate decreased for PVDF/PVP films as compared to neat PVDF films and was affected by the molecular weight of PVP. The results based on Ziabicki's model revealed that the addition of PVP decreased the ability of PVDF to crystallize under non-isothermal melt crystallization conditions. The activation energy was calculated through Friedman and advanced isoconversional methods. Results showed that the addition of PVP to PVDF films caused an increase in activation energy. By comparing DMTA results of PVDF/PVP blends with neat PVDF films, it could be concluded that blending PVDF with PVP caused an increase in the glass transition temperature ( $T_g$ ) while the storage modulus was decreased.

**Keywords:** Poly(vinylidene fluoride); Poly (N- vinylpyrrolidone); Crystallization kinetics; Non-isothermal crystallization; Differential scanning calorimetry.

## INTRODUCTION

Polyvinylidene fluoride is popular in industrial applications as a semi-crystalline polymer due to favorable properties like good thermal stability, chemical resistance, high mechanical strength and ferro-electricity (Nasir *et al.*, 2007; Sencadas *et al.*, 2010). The crystalline structures of PVDF polymer, according to the chain conformation with trans or gauche linkages, are  $\alpha$ ,  $\beta$  and  $\gamma$  phases (Nasir *et al.*,

2007). The crystalline morphology and crystallinity of PVDF are of major importance in various applications. However, the hydrophobic characteristic of PVDF is a limitation in some applications. For example, membrane fouling caused by hydrophobic interactions results in rapid water flux decline and high energy-consumption, especially when the wastewater contains natural organic matter (NOM), proteins and micro-organisms (Rajabzadeh *et al.*, 2012).

\*To whom correspondence should be addressed

Hydrophobic characteristics of polymers can be altered by polymer blending, that is more effective and widely used in comparison to chemical synthesis procedures (Ma *et al.*, 2008; Li and Xu, 2012; Li *et al.* 2013). Studies showed that the crystalline phase of PVDF can be changed by blending with amorphous polymers exhibiting physical interaction with PVDF. Therefore, it is necessary to investigate the crystallization kinetics for optimizing the process conditions and improving the structure-property correlation. The main focus has been on the crystallization behavior of PVDF and its blend in melt crystallization processes in the open literature (Lee and Ha, 1998; He *et al.*, 2008; Zhong *et al.*, 2011). Sencadas *et al.* (2010) studied the isothermal melt crystallization of PVDF at different crystallization temperatures. The Avrami parameters and the Hoffman-Weeks model were discussed to obtain the equilibrium melting temperature. The crystallization and morphological behavior of PVDF/polyhydroxybutyrate blends were also studied by Liu *et al.* (2005). They described a phase diagram by calorimetric measurements and reported the Avrami exponent for pure PVDF, which has a value of approximately three. The miscibility behavior of poly(methyl methacrylate) and PVDF was investigated by Fan *et al.* (2007). They found that the Avrami exponent decreases with rising crystallization temperature. Mancarella and Martuscelli (1977) also reported that the PVDF Avrami exponent variation was between 2.99 and 4.60 and that the half crystallization time was increased by an increase in crystallization temperature. Gradys *et al.* (2007) studied non-isothermal crystallization of PVDF at ultra high cooling rates. Their results indicated that pure  $\beta$ - phase of PVDF was obtained during the melt- crystallization process at cooling rates above 2000 K/s.

Although, there are some reports in the literature on the crystallization behavior of PVDF, less attention was paid to the non-isothermal crystallization kinetics of PVDF/PVP blends. In this study, the effect on PVDF crystallization of PVP with various molecular weights as an amorphous and water soluble polymer was investigated. The PVDF/PVP blend is a miscible system due to the compatibility of the two polymers (Chen and Hong, 2002; Ji *et al.*, 2008; Freire *et al.*, 2012). Dynamic mechanical thermal analysis (DMTA) was used to characterize the dynamic mechanical properties of PVDF films. The Jeziorny, Ozawa, Mo and Ziabicki kinetic models were applied to describe the crystallization behavior of PVDF films. Furthermore, the activation energy of melt crystallization for sample films was determined from the Friedman equation and advanced isoconversional method.

## MATERIALS AND METHODS

Poly(vinylidene fluoride) ( $M_w = 530000 \text{ gmol}^{-1}$ ) was purchased from Sigma-Aldrich (USA). Poly (N-vinylpyrrolidone) (PVP) (K 17,  $M_w 10,000 \text{ gmol}^{-1}$  and  $360000 \text{ gmol}^{-1}$ ) was provided by Rahavard Tamin Chemical Co. (Iran). N, N-Dimethylformamide (DMF) was obtained from Sigma-Aldrich (USA) and used as solvent. All chemicals were used without further purification.

### Sample Preparation

PVDF films were prepared using the solvent casting method. Poly(vinylidene fluoride) pellets were dissolved in DMF at  $50 \text{ }^\circ\text{C}$  for 10 h and then poly(N-vinylpyrrolidone) was added at a PVDF: PVP weight ratio of 1:1. The PVDF solution was poured into a flat dish for solvent evaporation at room temperature within an interval of two weeks. The samples were dried further at  $50 \text{ }^\circ\text{C}$  for 8 h to remove the solvent residues. The thicknesses of polymer films were about 150-200  $\mu\text{m}$ . The samples were named neat PVDF, PVDF/PVP1 for PVP with low molecular weight and PVDF/PVP2 for PVP with high molecular weight.

### Characterizations

The crystallization kinetics of PVDF polymer and the effects of PVP on its crystallization behavior were evaluated using a differential scanning calorimeter (DSC) (Polylab 625, instrument, UK). The weights of all samples were  $\sim 5 \text{ mg}$ . The samples were heated from room temperature to  $200 \text{ }^\circ\text{C}$  with a  $30 \text{ }^\circ\text{C min}^{-1}$  heating rate and held for 3 min to eliminate the previous thermal history. Subsequently, the samples were cooled to  $50 \text{ }^\circ\text{C}$  at predetermined rates. The non-isothermal process included melt crystallization at different cooling rates: 2.5, 5, 10 and  $20 \text{ }^\circ\text{C min}^{-1}$ , while exothermal curves of heat flow were recorded as a function of temperature and the experiments carried out under nitrogen atmosphere. FTIR spectra were obtained by a FTIR instrument (Bruker, model Equinox) in the  $600\text{--}3500 \text{ cm}^{-1}$  wave number range. Dynamic mechanical thermal analyses of the samples were carried out using a DMA, (Tritec 2000 machin) under the bending mode at a frequency of 0.1 Hz. The temperature range was from  $-100$  to  $100 \text{ }^\circ\text{C}$  at a rate of  $5 \text{ }^\circ\text{C min}^{-1}$ . The dried polymer films were cut into approximately  $2.5 \times 1 \times 0.15 \text{ cm}^3$  rectangles. The amplitude was set to be within the linear viscoelastic regime.

## RESULTS AND DISCUSSION

### Non-isothermal Crystallization Behavior

Crystallization in miscible blends similar to pure polymers was limited to temperatures between the glass transition temperature and the equilibrium melting point. In this study, PVDF as a semi-crystalline polymer was blended with PVP. Crystallization rates in such blends were different from pure PVDF due to the dilution of crystallizable chain.

Non-isothermal melt crystallization thermograms of neat PVDF films and PVDF/PVP blends at various cooling rates and melting behaviors at  $10\text{ }^{\circ}\text{C min}^{-1}$  heating rate after non-isothermal crystallization are shown in Figure 1. All experimental data for PVDF/PVP2 are presented in Table 1. From the melting curves of neat PVDF, PVDF/PVP1 and PVDF/PVP2 films (Fig. 1), the temperature peak position remained constant during the heating process.

The melting behavior of crystallized PVDF films showed the fusion endotherms to be around 160, 155 and  $145\text{ }^{\circ}\text{C}$  for neat PVDF, PVDF/PVP1 and PVDF/PVP2 films, respectively. As can be seen, there is a single endothermal melting during the second heating run. However, the peak at the lower heating rate (that is,  $2.5\text{ }^{\circ}\text{C min}^{-1}$ ) showed a small shoulder in front of the melting. It could be related to the recrystallization of PVDF during the heating process since various cooling rate settings does not influence the two melting peaks. Similar results were obtained by Ma *et al.* (2011).

The data presented in Fig. 1 are listed in Table 1. In this table, the total crystallization enthalpies ( $\Delta H_c$ ), the onset ( $T_c^{on}$ ), peak ( $T_c^P$ ) and end ( $T_c^f$ ) crys-

tallization temperatures are shown for PVDF films. The results showed that  $T_c^P$  shifted to lower temperatures for the samples as the cooling rate increased.

It can be inferred that the PVDF molecules reorganize and form stable nuclei at a slower cooling rate. On the other hand, at high cooling rate the motion of the chain segments of PVDF could not follow the cooling rate; so, more supercooling was needed to initiate crystallization (Bianchi *et al.*, 2014; Xiong *et al.*, 2007). According to Fig. 1, the crystallization temperatures (including the values of  $T_c^{on}$ ,  $T_c^P$  and  $T_c^f$ ) of PVDF/PVP samples are lower than those of neat PVDF films. The  $T_c^P$  values for PVDF containing higher molecular weight PVP (PVDF/PVP2) decrease more than for PVDF/PVP1. In addition, the presence of PVP in the PVDF film leads to a widening of the crystallization peaks.

It can be seen that the values of  $\Delta H_c$  decreased with an increase in the cooling rate. The total crystallization enthalpies of neat PVDF films were slightly influenced by cooling rate. However, the value of  $\Delta H_c$  decreased significantly for PVDF/PVP blends in comparison with neat PVDF films. This may be related to reduction in the amount of crystals formed and a lower degree of perfection of the crystals.

Based on the results, PVP has a negative influence on the crystallinity of PVDF films. This can be explained by interaction of functional groups of PVDF and PVP through hydrogen bonding interactions. The hydrogen bonding occurs between the carbonyl group of PVP and the methylene group of PVDF due to the acidity of PVDF hydrogen atoms and the electronegativity of PVP oxygen atoms (Chen and Hong, 2002). This interaction suggests restricted movement of the PVDF chains.

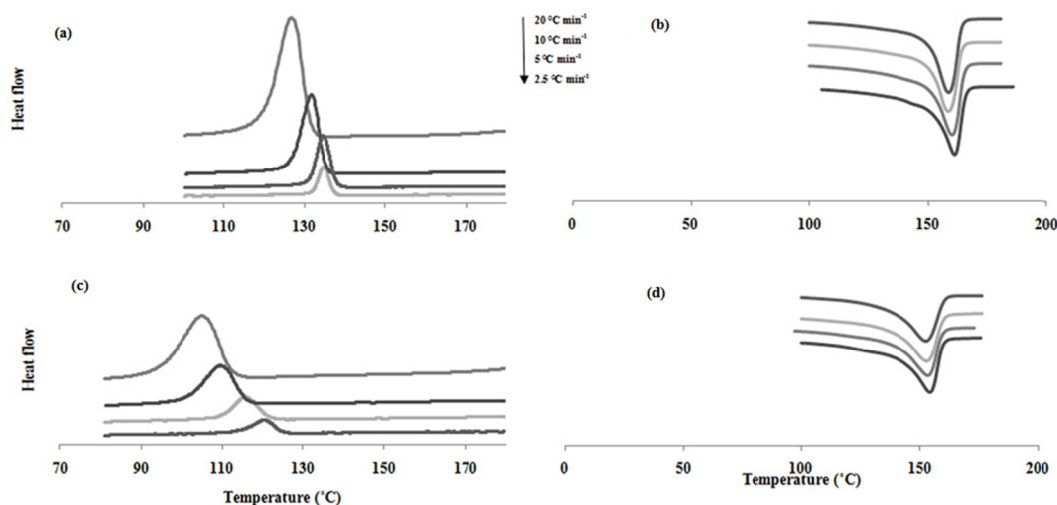


**Figure 1:** The DSC curves of non-isothermal crystallization at different cooling rates (a and c) and those of melting behaviors at a heating rates of  $10\text{ }^{\circ}\text{C min}^{-1}$  after crystallization (b and d) of neat PVDF and PVDF/PVP1 films.

**Table 1: Characteristic data of the non-isothermal crystallization behavior for neat PVDF and PVDF/PVP films.**

Sample	$\phi$ ( $^{\circ}\text{C min}^{-1}$ )	$T_c^{on}/^{\circ}\text{C}$	$T_c^p/^{\circ}\text{C}$	$T_c^f/^{\circ}\text{C}$	$\Delta T_c$	$\Delta H_c$ ( $\text{Jg}^{-1}$ )
PVDF	2.5	137.4	134.8	132.1	18.8	36.49
	5	138	134.7	131.2	22.5	36.41
	10	135.3	132	126.8	23.5	36.11
	20	131	126	119.6	27.8	35.95
PVDF/PVP1	2.5	124.8	120.4	114.2	29.7	34.1
	5	121.5	115.7	109.6	34.8	30.3
	10	116	109.6	100.8	36.8	33.84
	20	112.4	105	94.1	40	32.5
PVDF/PVP2	2.5	89	102.2	113	56.5	30.92
	5	83	96.9	111	60.2	27.28
	10	73	93.9	108	71.8	26.64
	20	60	85	104	81.5	14.67

### FTIR Spectroscopy

For a better understanding of interaction between PVDF and PVP in PVDF/PVP blends, FTIR spectroscopy was used. Fig. 2 shows spectra of neat PVDF and its blends. The absorption bands at 1395 and 890  $\text{cm}^{-1}$  are attributed to the C–F vibration and at 1160  $\text{cm}^{-1}$  assigned to the C–C bond (Fig. 2a). From the FTIR spectra, crystalline PVDF phases can be identified by the absorption bands (Martin *et al.*, 2012). The  $\beta$  phase is assigned at 828 and 1063  $\text{cm}^{-1}$ , and the absorption bands at 602 and 1225  $\text{cm}^{-1}$  are characteristic of  $\alpha$  and  $\gamma$  phases, respectively.

From Fig. 2 it can be seen that the carbonyl stretching absorption band of PVP assigned at 1638  $\text{cm}^{-1}$  in pure PVP shifted to 1662  $\text{cm}^{-1}$  and 1691  $\text{cm}^{-1}$  in PVDF/PVP1 and PVDF/PVP2 films, respectively. This shift toward higher frequency can be explained by the effect of the hydrogen bond formed between the carbonyl group of PVP and the methylene group of PVDF. The same result was reported by Chen and Hong (2002).

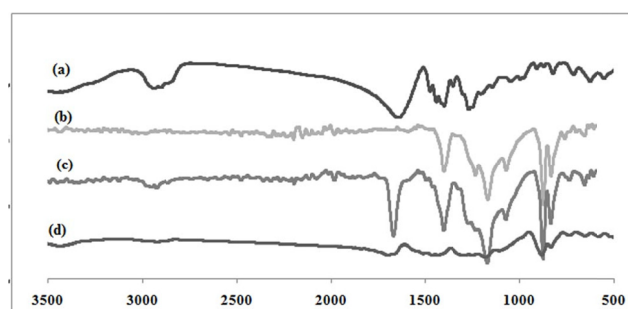


**Figure 2:** FT-IR spectra of neat PVDF and PVDF/PVP films: pure PVP (a), neat PVDF (b), PVDF/PVP1 (c) and PVDF/PVP2 (d).

### Dynamic Mechanical Thermal Analysis

Viscoelastic properties of the materials could be measured by the dynamic mechanical thermal technique. In dynamic mechanical thermal analysis (DMTA), stiffness (E-modulus) and the damping effect, which are two important viscoelastic properties, are evaluated as a function of temperature and frequency. The presence of a second polymeric component in semi-crystalline polymers changes the mobility of the polymer chains that can be observed by the change of the modulus and glass transition temperature ( $T_g$ ) of the polymer (Badia *et al.*, 2014). In practice,  $T_g$  determines the temperature at which a maximum in the mechanical damping parameter ( $\tan \delta$ ) or loss modulus ( $E''$ ) occurs. In this study, the effect of PVP on the amorphous region of PVDF was determined by evaluating dynamic property changes using DMTA. Two relaxation processes such as segmental molecular motions and local motions of small groups in the chain occurred during the PVDF heating process (Lobo and Bonilla, 2003; Osinska *et al.*, 2013).

Fig. 3 shows the storage modulus ( $E'$ ) and  $\tan \delta$  vs. temperature of neat PVDF, PVDF/PVP1 and PVDF/PVP2 samples in the temperature range of  $T = -150$  to 100  $^{\circ}\text{C}$  at 0.1 Hz. From Fig. 3a, it is observed that an increase in temperature caused a decrease in the  $E'$  values of polymeric films. The storage modulus of PVDF films containing PVP with high molecular weight decreased compared with neat PVDF due to the lower crystallinity. It could be considered that the presence of PVP in the films reduced the intermolecular dipole bonding of PVDF chains.

Lobo and Bonilla (2003) have reported that the  $T_g$  and relaxation process associated with the crystalline

fraction molecular motions of PVDF occurred at -42 and 86 °C, respectively. The maximum value of the  $\tan \delta$  curve (Fig. 3b), which is defined as the  $T_g$  of neat PVDF film is -40 °C. For PVDF/PVP films, this value is shifted to higher temperatures (-8 and 35 °C for PVDF/PVP1 and PVDF/PVP2, respectively). The shift of  $T_g$  to higher temperatures confirmed the decrease in the mobility of the PVDF chains in the presence of PVP, as described previously.

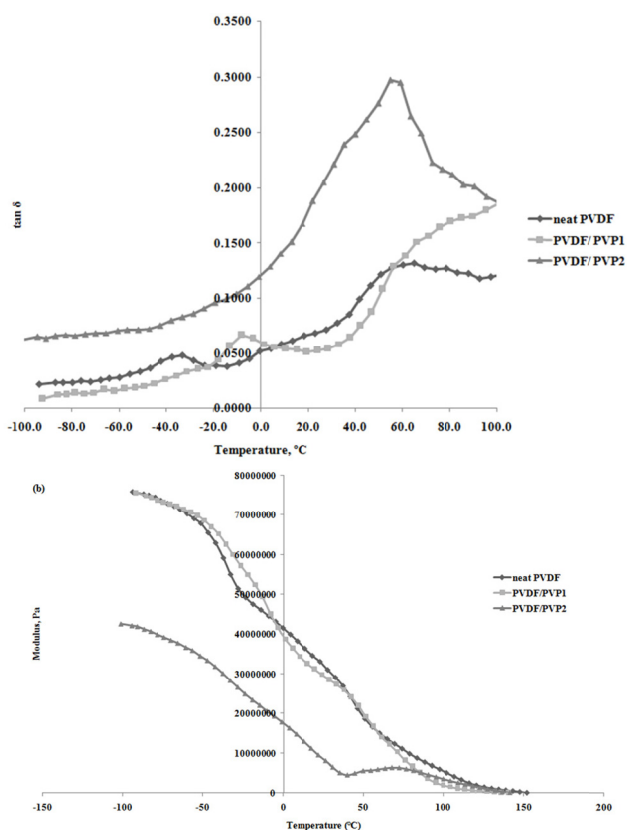


**Figure 3:** The  $\tan \delta$  (a) and storage modulus (b) versus temperature of neat PVDF and PVDF/PVP samples.

### Crystallizability of PVDF

A simple method to evaluate the crystallizability of polymers and their sensitivity to processing conditions was developed by Nadkarni *et al.* (1993). Accordingly, the variation in the degree of undercooling ( $\Delta T_c$ ) with cooling rate ( $\phi$ ) can be expressed as:

$$\Delta T_c = P\phi + \Delta T_c^0 \quad (1)$$

where  $\Delta T_c^0$  is the degree of undercooling required in the limit of zero cooling rate and the slope  $P$  is a process sensitivity factor.  $\Delta T_c^0$  is associated with the thermodynamic driving force for nucleation and the  $P$  factor accounts for the kinetic effects (Lorenzo *et*

*al.*, 1999; Song *et al.*, 2011).  $\Delta T_c$  was considered to be the difference between  $T_c^{on}$  and  $T_m$  in the subsequent heating scan (Table 1). The variations of the degree of supercooling with the cooling rate show the ability of the polymer molecules to respond to the changes in the thermal conditions. Thus, the slope of the line of  $\Delta T_c$  vs. cooling rate is the process sensitivity factor.

Fig. 4 shows the plots of variation of  $\Delta T_c$  with cooling rate. The values of  $\Delta T_c^0$  can be obtained from the intercepts to evaluate the crystallizability of the blends. The results show that the  $\Delta T_c^0$  values increased from 18.8 for neat PVDF to 30.5 for PVDF/PVP1 and 53.9 for PVDF/PVP2. Such an increase suggests that the thermodynamic driving force for nucleation of PVDF is significant after the addition of PVP. The values of the  $P$  factor followed the order: PVDF/PVP2 > PVDF/PVP1 > neat PVDF films. These results show that PVP reduced the crystallization of PVDF in the blend films.

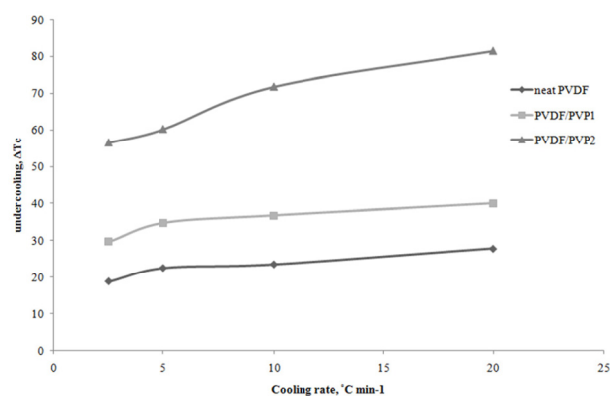


**Figure 4:** Variation of  $\Delta T_c$  with cooling rate for neat PVDF and PVDF/PVP films.

### Relative Crystallinity of PVDF

The relative degree of crystallinity ( $X(t)$ ) as a function of the crystallization temperature or time was determined from the crystallization exotherms of polymers by partial integration of crystallization exotherms.  $X(t)$  is defined as a function of temperature:

$$X(t) = \frac{\int_{T_0}^T \left( \frac{dH_c}{dT} \right) dT}{\int_{T_0}^{T_\infty} \left( \frac{dH_c}{dT} \right) dT} \quad (2)$$

where  $T_0$  and  $T_\infty$  are the onset and end crystallization temperatures, respectively.

For the non-isothermal crystallization process, the relationship between crystallization time ( $t$ ) and the

corresponding temperature ( $T$ ) can be expressed as follows:

$$t = \frac{T - T_0}{\phi} \quad (3)$$

where  $\phi$  is the cooling rate (Ji *et al.*, 2008). The horizontal temperature axis can be transformed into a time scale. Fig. 5 shows the variations of relative crystallinity with crystallization time for neat PVDF and PVDF/PVP films. All these curves have the same characteristic sigmoidal shape at various cooling rates due to the spherulite impingement in the later stage of crystallization. It can be seen that, for crystallization completion, a shorter time requires higher cooling rates.

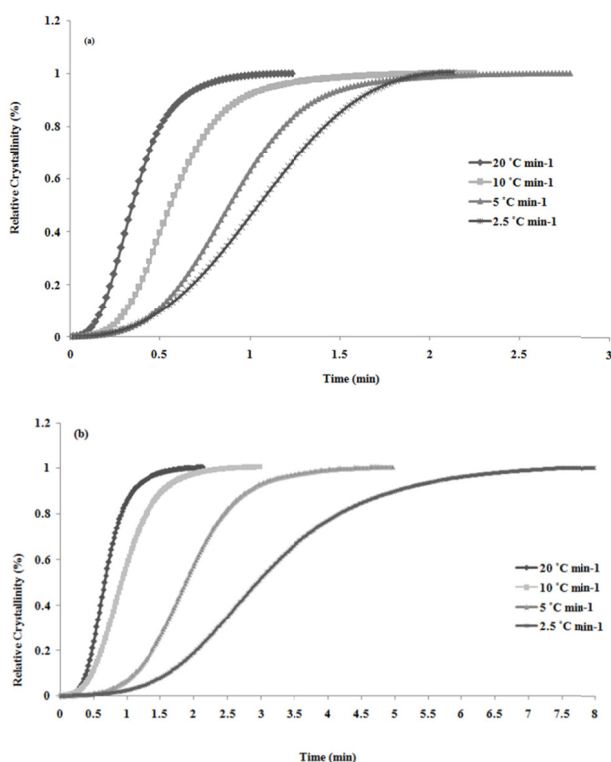


**Figure 5:** Relative crystallinity versus time for neat PVDF (a) and PVDF/PVP1 (b) films at various cooling rates.

### Non-Isothermal Crystallization Kinetics Analysis

#### Modified Avrami Model (Jeziorny Equation)

Several methods have been developed to describe the non-isothermal crystallization kinetics of polymers. The Avrami equation was used to describe the primary stages of isothermal kinetics. According to the model, the relative crystallinity ( $X(t)$ ) changes with crystallization time ( $t$ ) as follows:

$$X(t) = 1 - \exp(-kt^n) \quad (4)$$

where  $k$  and  $n$  are the crystallization rate constant and the Avrami exponent, respectively (Ji *et al.*, 2008).

In actual conditions, the temperature changes constantly during non-isothermal crystallization; hence, the parameters  $n$  and  $k$  have different physical meanings. Therefore, Jeziorny considered the correction of the crystallization rate constants by introducing the cooling rate. The modified equation is expressed by (Jeziorny, 1978):

$$\log Z_c = \frac{\log Z_t}{\phi} \quad (5)$$

where  $Z_c$  is the modified crystallization rate constant and  $Z_t$  is the rate constant of the non-isothermal crystallization process (Yu *et al.*, 2009; Bahader *et al.*, 2015; Lang and Zhang, 2013). The values of  $Z_c$  are shown in Table 2.  $Z_c$  is increased by increasing the cooling rate. The modified crystallization rate constant of PVP loaded PVDF films decreased to some extent, in contrast to that of neat PVDF, at various cooling rates.

The crystallization half-time ( $t_{1/2}$ ), is defined as the time ( $t$ ) at which the extent of crystallization reaches 50%.  $t_{1/2}$  for non-isothermal crystallization can be obtained from Equation 6 and used to evaluate non-isothermal crystallization rates. The data are shown in Table 2. Generally, short  $t_{1/2}$  means faster crystallization processes. The  $t_{1/2}$  values indicate that the higher cooling rates have shorter crystallization completion times for both neat and PVDF/PVP films. Moreover, the values of  $t_{1/2}$  for neat PVDF films are lower in comparison to those of PVDF/PVP films.

$$t_{1/2} = \left( \frac{\ln 2}{k} \right)^{1/n} \quad (6)$$

Obviously, the data show that PVP influenced the kinetic parameters  $Z_c$  and  $t_{1/2}$ . Thus, the PVDF crystallization rate was reduced upon blending with PVP. As discussed earlier, this effect was caused by reducing PVDF molecular mobility due to stronger interactions with PVP in the molten state. The results show that the crystallization rate of PVDF was affected more by PVP with higher molecular weight due to more interactions of the PVDF and PVP polymer chains.

**Table 2: Crystallization kinetic parameters of neat PVDF and PVDF/PVP films.**

Sample	$\Phi$ ( $^{\circ}\text{Cmin}^{-1}$ )	$Z_c$ ( $^{\circ}\text{Cmin}^{-1}$ )	$t_{1/2}$ (min)	$T_{max}$ ( $^{\circ}\text{C}$ )	$(dX(t)/dt)_{max}$ ( $\text{s}^{-1}$ )	$D_{\phi}$ ( $^{\circ}\text{C}$ )	$G_{z,\phi}$ ( $^{\circ}\text{C min}^{-1}$ )	$G_z$
Neat PVDF	2.5	0.88	0.98	135.1	0.014	2.69	2.53	1.01
	5	0.97	0.91	134.7	0.019	3.9	4.95	0.99
	10	1.12	0.58	132.0	0.030	5.01	9.69	0.96
	20	1.12	0.35	127.0	0.042	6.88	18.83	0.94
PVDF/PVP1	2.5	0.23	2.99	120.9	0.008	6.3	2.33	0.93
	5	0.59	1.93	115.8	0.010	6.89	4.74	0.94
	10	0.98	0.93	109.7	0.017	8.61	9.50	0.95
	20	1.05	0.66	104.8	0.027	10.47	18.04	0.90
PVDF/PVP2	2.5	0.24	4.01	103.4	0.003	11.8	2.41	0.96
	5	0.58	2.69	99.4	0.005	11.2	4.15	0.83
	10	0.88	1.56	93.9	0.008	14.9	7.64	0.76
	20	0.95	1.25	88.1	0.010	25.1	17.30	0.86

### Ozawa Method

The Ozawa model is one of the most used kinetic approaches for non-isothermal crystallization process, proposed by extending the Avrami Equation (Jeziorny, 1978). This model is based on the assumption that the non-isothermal crystallization process can be divided into small isothermal steps. The Ozawa Equation is expressed as:

$$X(t) = 1 - \exp\left[\frac{-K(T)}{\phi^m}\right] \quad (7)$$

$$\ln[-\ln(1 - X(t))] = \ln K(T) - m \ln \phi \quad (8)$$

where  $K(T)$  and  $m$  are the cooling function and the Ozawa exponent, respectively. The Ozawa exponent depends on the dimension of crystal growth. Plots of  $\ln[-\ln(1 - X(t))]$  versus  $\ln \phi$  are shown in Figure 6.

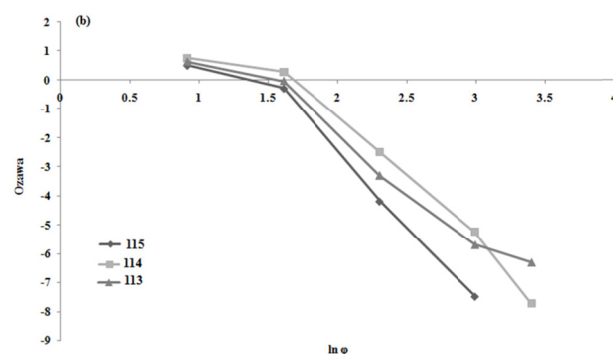
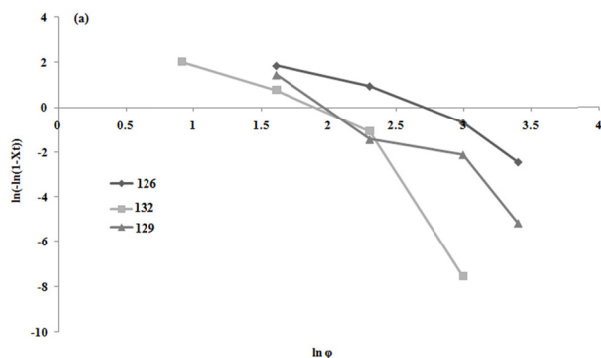


**Figure 6:** The Ozawa plots of neat PVDF (a) and PVDF/PVP1 (b) films.

It can be seen that these figures have poor linear correlations. Changes in slopes indicate that  $m$  varies with temperature. Thus, the Ozawa method was not satisfactory for the description of the crystallization kinetics of PVDF films. Some authors have declared that the Ozawa model cannot be applied for modeling the crystallization kinetics of polymers that have secondary crystallization (Ozawa, 1971; Yu. *et al.*, 2009).

### Combined Avrami and Ozawa Equations (Mo Model)

It is obvious that the Avrami analysis and its Jeziorny modification could only describe the primary stages of non-isothermal melt crystallization. In order to find a method to describe the non-isothermal crystallization process exactly, Mo and his colleagues suggested a new method (Liu *et al.*, 1997; Qiu *et al.*, 2000). This method is the combination of the Avrami and Ozawa Equations at a given value of  $X(t)$ :

$$\ln \phi = \ln F(T) - \alpha \ln t \quad (9)$$

where  $F(T) = [K(T)/Z_t]^{1/m}$  refers to the value of the cooling rate and  $\alpha$  is the ratio of  $n$  to  $m$ .  $F(T)$  has a definite physical and practical meaning. At a given degree of crystallinity, the plots of  $\ln \phi$  versus  $\ln t$  yield a linear relationship for a certain relative degree of crystallinity, as shown in Fig. 7. It can be seen that the Mo model was successful in describing the non-isothermal process of neat PVDF, PVDF/PVP1 and PVDF/PVP2 films. The values of  $\alpha$  and  $F(T)$  can be calculated from the slope and the intercept of the lines. The kinetic parameters are listed in Table 3.

**Table 3: The kinetic parameters from the Mo model.**

Sample	$X(t)$ %	$\alpha$	$F(T)$
Neat PVDF	20	0.58	5.31
	40	1.03	5.73
	50	1.20	6.09
	80	1.79	7.41
PVDF/PVP1	20	1.31	6.75
	40	1.37	9.58
	50	1.38	11.0
	80	1.42	17.98
PVDF/PVP2	20	1.63	12
	40	1.75	22.9
	50	1.65	27.32
	80	1.67	47.7

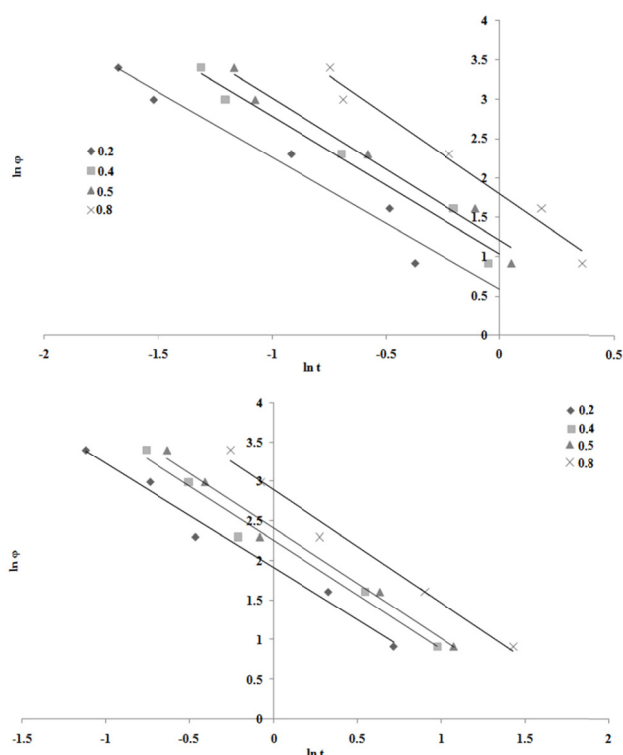


**Figure 7:** Plots of  $\ln \phi$  versus  $\ln t$  for neat PVDF (a) and PVDF/PVP1 (b) films.

The values of  $\alpha$  vary from 1.62 to 2.07 for neat PVDF and 1.31 to 1.7 for PVDF/PVP films. The data show that  $F(T)$  increased upon increasing the relative crystallinity. On the other hand, PVDF films containing PVP revealed higher  $F(T)$  values as compared to the values achieved for neat PVDF films at the same  $X(t)$  values. Since  $F(T)$  reflects the difficulty of the crystallization process, at similar  $X(t)$  values, the higher  $F(T)$  values for PVP loaded PVDF films is in accordance with slower crystallization rates. It is found that  $F(T)$  values are higher for PVDF/PVP2 films. This is also in agreement with other kinetic parameters.

### Analysis Based on Ziabicki Model

Ziabicki developed another approach for non-isothermal crystallization kinetics related to the crystallization progress and crystallization rate-temperature function (Ziabicki, 1996). Crystallization kinetics of polymers in Ziabicki's model can be described by the following equation (first order kinetics):

$$\frac{dX(t)}{dt} = K_Z(T)[1 - X(t)] \quad (10)$$

where  $K_Z(T)$ , the crystallization rate function, can be expressed by:

$$K_Z(T) = K_{Z,\max} \exp \left[ -4 \ln 2 \frac{(T - T_{\max})^2}{D^2} \right] \quad (11)$$

where  $T_{\max}$ ,  $K_{Z,\max}$  and  $D$  are the maximum crystallization rate temperature, the crystallization rate at  $T_{\max}$  and the width at half-height measured from the crystallization rate function, respectively. With the isokinetic approximation, the semi-crystalline polymer crystallization ability (kinetic crystallizability index),  $G_Z$ , was obtained by the integration of Equation (11) over the crystallization range:

$$G_Z = \int_{T_g}^{T_m} K_Z(T) dT \approx 1.064 K_{Z,\max} D. \quad (12)$$

The  $G_Z$  parameter expresses the ability of a semi-crystalline polymer to crystallize. In the case of non-isothermal crystallization studies using DSC,  $K_Z(T)$  can be replaced in Equation (12) with the derivative function of the relative crystallinity,  $(dX/dT)_\phi$ , for each cooling rate study as follows:

$$G_{Z,\phi} = \int_{T_g}^{T_m} (dX/dT)_\phi dT \approx 1.064 (dX/dT)_{\phi,\max} D_\phi \quad (13)$$



where  $(dX/dT)_{\phi, \max}$ ,  $D_{\phi}$  and  $G_{z, \phi}$  are the maximum crystallization rate, the width at half-height of the  $(dX/dT)_{\phi}$  function and the kinetic crystallizability index for an arbitrary cooling rate. The Ziabicki kinetic crystallizability index,  $G_z$ , can be obtained by  $G_{z, \alpha}$  normalization with  $\phi$  (i.e.,  $G_z = G_{z, \phi}/\phi$ ) (Supaphol *et al.*, 2004). Table 2 summarizes the crystallization kinetics parameters of neat PVDF and PVDF/PVP films based on Ziabicki's model. The values of  $T_{\max}$  decreased, while  $(dX/dT)_{\phi, \max}$ ,  $D_{\phi}$  and  $G_{z, \phi}$  increased with increasing cooling rate. The average values of  $G_z$  for neat PVDF and PVDF/PVP1 and PVDF/PVP2 films were 1.006, 0.933 and 0.835, respectively. The reduction of the  $G_z$  value for PVDF/PVP films shows that PVP decreased the ability of PVDF to crystallize under non-isothermal melt crystallization conditions.

### Effective Activation Energy

Several methods such as Kissinger, Vyazovkin and Friedman methods are used to evaluate the activation energy for the crystallization process (Kissinger, 1956; Vyazovkin, 2002; Friedman, 1964; Omrani *et al.*, 2013). In fact, the activation energy was closely related to the relative crystallinity degree. In order to calculate approximately reliable values of the effective activation energy, the differential isoconversional method of Friedman and the advanced integral isoconversional method of Vyazovkin were used.

### Friedman Equation

The Friedman Equation is expressed as follows (Ma *et al.*, 2011; Friedman, 1964):

$$\ln\left(\frac{dX(t)}{dt}\right)_{X(t)} = \text{constant} - \frac{E_{X(t)}}{RT_{X(t)}} \quad (14)$$

where  $dX(t)/dt$  is the instantaneous crystallization rate as a function of time ( $t$ ) for a given value of relative crystallinity ( $X(t)$ ),  $R$  is the gas constant, and  $E_{X(t)}$  the effective energy barrier of the process for a given value of  $X(t)$ . A straight line can be obtained by plotting  $dX(t)/dt$  versus  $1/T_{X(t)}$ . The slope of plot is equal to  $-E_{X(t)}/R$ . Thus, the activation energy ( $E_{X(t)}$ ) can be calculated from the slope of the straight line.

Fig. 8 illustrates plots of effective activation energy as a function of relative crystallinity for neat PVDF and PVP loaded PVDF samples. According to the results, the activation energy increased upon increasing the relative crystallinity, suggesting that

the crystallization becomes more difficult with an increase in relative crystallinity. Indeed, one should expect that transmission of the polymer segments from the equilibrium melt to the growth front will be slowed down as crystallization proceeds. It is also observed that the calculated activation energy values varied in the following manner: neat PVDF < PVDF/PVP1 < PVDF/PVP2 films, indicating that PVP caused a delay in the crystallization process of PVDF polymer.

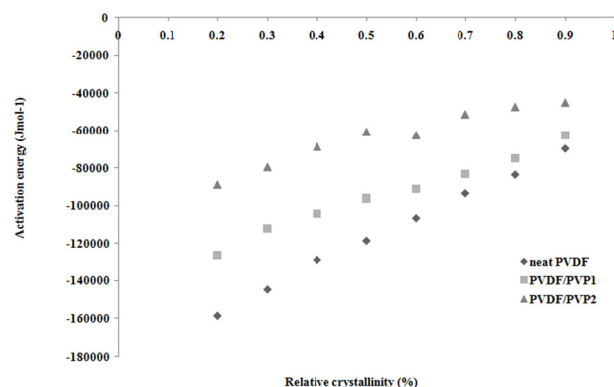


**Figure 8:** Plots of effective activation energy as a function of relative crystallinity for neat PVDF and PVDF/PVP films using the Friedman equation.

### Advanced Isoconversional Method

It is noteworthy that the sole dependence of the activation energy on relative crystallinity is sufficient to reliably predict the behavior of a substance. The accuracy of such predictions obviously depends on the accuracy of calculating the activation energy. Thus, errors in computing the activation energy must be minimized. One of the sources of these errors are approximations intentionally used to derive the linear final plots yielding the activation energy. Approximations undeniably induced an error in the values of the activation energies. To resolve this problem, a non-linear procedure for computing the activation energy by the isoconversional method was developed. An advanced isoconversional method (non-linear) was described by Vyazovkin (1997). In the present study, a non-linear isoconversional method was applied to the dynamic DSC data of neat PVDF system using the following equation:

$$\Phi(E_a) = \sum_{i=1}^n \sum_{j \neq i}^n \frac{I(E_a, T_{a,i}) \phi_j}{I(E_a, T_{a,j}) \phi_i} \quad (15)$$

where  $\phi$  is the cooling rate,  $T$  is the temperature,  $E_a$  is the activation energy,  $i, j$  are the ordinal

numbers of DSC runs performed at different cooling rates. The activation energy can be found at any particular conversion level by finding the value of  $E_a$  at which the  $\Phi(t)$  function has a minimum value. In Equation (12) the temperature integral was determined by the Senum-Yang approximation (Senum *et al.*, 1977) given as:

$$I(E_a, T) = \int_0^{T\alpha} \exp\left(\frac{E_a}{RT}\right) dT \quad (16)$$

$$I(E_a, T) = \left(\frac{E_a}{R}\right) P(x) \quad (17)$$

and

$$P(x) = \frac{\exp(-x)}{x} \left( \frac{x^3 + 18x^2 + 88x + 96}{x^4 + 20x^3 + 120x^2 + 240x + 120} \right) \quad (18)$$

Each value of  $X(t)$  was minimized to obtain the  $E_a$  dependence. The advanced isoconversional method applied the same computational algorithm for isothermal and non-isothermal DSC data. The isoconversional plot trends in Fig. 9 are similar to those obtained from the Friedman method.

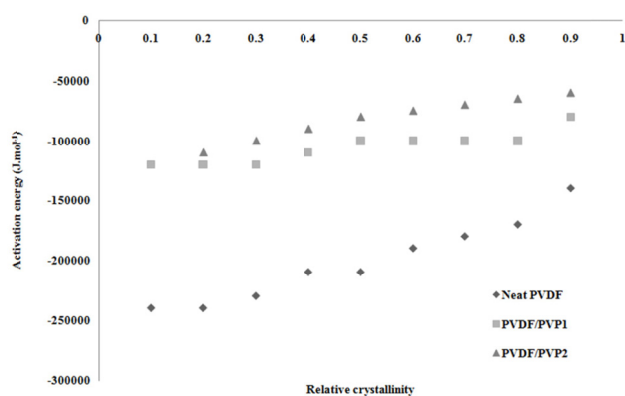


**Figure 9:** Plots of effective activation energy as a function of relative crystallinity for neat PVDF and PVDF/PVP films using the advanced isoconversional method.

## CONCLUSIONS

The non-isothermal melt crystallization kinetics of PVDF and its blends with PVP were studied at various cooling rates using DSC. As compared with neat PVDF, PVDF/PVP blends exhibit reduced crystallization ability due to the tendency of PVDF to

interact with PVP through hydrogen bonding between the hydrogen atoms of PVDF and oxygen atoms of the carbonyl groups in PVP. The effect of PVP on the glass transition temperature of PVDF was also evaluated by DMTA analysis. It has been found that PVDF films containing PVP have higher  $T_g$  values in comparison to neat PVDF films. The Jeziorny, Mo and Ziabicki models were applied to describe the crystallization process and appeared to be successful. The Ozawa equation was found to be invalid for describing the crystallization kinetics. Kinetic parameters obtained from these mathematical models showed that the crystallization rate of PVDF decreased in the presence of PVP and was affected by the molecular weight of PVP. The activation energies of melt crystallization for PVDF and PVDF/PVP blends were determined according to Friedman and advanced isoconversional methods. The higher value of the activation energy for PVDF/PVP blends compared to neat PVDF was also consistent with the lower rate of crystallization.

## REFERENCES

- Badia, J. D., Santonja-Blasco, L., Martínez-Felipe, A., Ribes-Greus, A., Dynamic Mechanical Thermal Analysis of Polymer Blends, in Characterization of Polymer Blends: Miscibility, Morphology and Interfaces. (Eds. Thomas, S., Grohens, Y., Jyotishkumar, P.), Wiley-VCH Verlag GmbH & Co. KGaA, Weinheim, Germany, (2014).
- Bahader, A., Gui, H., Li, Y., Xu, P., Ding, Y., Crystallization kinetics of PVDF filled with multi wall carbon nanotubes modified by amphiphilic ionic liquid. *Macromol. Res.*, 23, 273 (2015).
- Bianchi, O., Martins, J. N., Luvison, C., Echeverrigaray, S. G., Dal Castel, C., Oliveira, R. V. B., Melt crystallization kinetics of polyhedral oligomeric silsesquioxane under non-isothermal conditions. *J. Non-Cryst. Solids*, 394, 29 (2014).
- Chen, N. P. and Hong, L., Surface phase morphology and composition of the casting films of PVDF–PVP blend. *Polymer*, 43, 1429 (2002).
- Fan, W., Zheng, S., Miscibility and crystallization behavior in blends of poly(methyl methacrylate) and poly(vinylidene fluoride): Effect of star-like topology of poly(methyl methacrylate) chain. *J. Polym. Sci., Part B*, 45, 2580 (2007).
- Freire, E., Bianchi, O., Martins, J. N., Monteiro, E. E. C., Forte, M., Non-isothermal crystallization of PVDF/PMMA blends processed in low and high shear mixers. *J. Non-Cryst. Solid.*, 358, 2674 (2012).

- Friedman, H. L., Kinetics of thermal degradation of char-forming plastics from thermogravimetry. Application to a phenolic plastic. *J. Polym. Sci. C: Polym. Sympos.*, 6, 183 (1964).
- Gradys, A., Sajkiewicz, P., Adamovsky, S., Minakov, A., Schick, C., Crystallization of poly(vinylidene fluoride) during ultra-fast cooling. *Thermochim. Acta*, 461, 153 (2007).
- He, F., Fan, J. and Lau, S., Thermal, mechanical and dielectric properties of graphite reinforced poly(vinylidene fluoride) composite. *Polym. Test.*, 27, 964 (2008).
- Jeziorny, A., Parameters characterizing the kinetics of the kinetics of the non-isothermal crystallization of poly (ethylene terephthalate) determined by DSC. *Polymer*, 19, 1142 (1978).
- Ji, G. L., Zhu, B. K., Zhang, C. F., Xu, Y. Y., Non-isothermal crystallization kinetics of poly(vinylidene fluoride) in a poly(vinylidene fluoride)/dibutyl phthalate/ di(2-ethylhexyl)phthalate system via thermally induced phase separation. *J. Appl. Polym. Sci.*, 107, 2109 (2008).
- Kissinger, H. E., Variation of peak temperature with heating rate in different thermal analysis. *J. Res. Natl. Bur. Stan.*, 57, 217 (1956).
- Lang, M., Zhang, J., Non-isothermal crystallization behavior of poly(vinylidene fluoride)/ethylene-vinyl acetate copolymer blends. *Iran. Polym. J.*, 22, 821 (2013).
- Lee, W. K. and Ha, C. S., Miscibility and surface crystal morphology of blends containing poly (vinylidene fluoride) by atomic force microscopy. *Polymer*, 39, 7131 (1998).
- Li, J., Wu, X. Liu, Z., Non-Isothermal crystallization of poly(vinylidene fluoride)/multiwalled carbon nanotube composites. *Int. J. Polym. Anal. Ch.*, 18, 83 (2013).
- Li, J. W., Xu, X. H., Non-Isothermal crystallization of poly(vinylidene fluoride)/hollow glass microspheres composites. *Polym.-Plast. Technol.*, 51, 1204 (2012).
- Liu, J., Qiu, Z. and Jungnickel, B. J., Crystallization and morphology of poly(vinylidene fluoride)/poly (3-hydroxybutyrate) blends. III. Crystallization and phase diagram by differential scanning calorimetry. *J Polym. Sci. B: Polym. Phys.*, 43, 287 (2005).
- Liu, Z., Mo, Z., Wang, S., Zhang, H., Non-isothermal melt and cold crystallization kinetics of poly(aryl ether ether ketone), *Polym. Eng. Sci.*, 37, 568 (1997).
- Lobo, H., Bonilla, J. V., *Handbook of Plastics Analysis*. CRC Press, Marcel Dekker, Inc (2003).
- Lorenzo, M. D., Silvestre, C., Non-isothermal crystallization of polymers. *Prog. Polym. Sci.*, 24, 917 (1999).
- Ma, W., Wang, X. and Zhang, J., Crystallization kinetics of poly(vinylidene fluoride)/MMT, SiO<sub>2</sub>, CaCO<sub>3</sub>, or PTFE nanocomposite by differential scanning calorimeter. *J. Therm. Anal. Calorim.*, 103, 319 (2011).
- Ma, W., Zhang, J. and Wang, X., Crystallization and surface morphology of poly(vinylidene fluoride)/poly(methylmethacrylate) films by solution casting on different substrates. *Appl. Surf. Sci.*, 254 (2008).
- Mancarella, C. and Martuscelli, E., Crystallization kinetics of poly(vinylidene fluoride) . *Polymer*, 18, 1240 (1977).
- Martins, J. N., Bassani, T. S., Oliveira, R. V. B., Morphological, viscoelastic and thermal properties of poly(vinylidene fluoride)/POSS nanocomposites. *Mater. Sci. Eng., C*, 32, 146 (2012).
- Nadkarni, V., Bulakh, N., Jog, J., Assessing polymer crystallizability from nonisothermal crystallization behavior. *Adv. Polym. Technol.*, 12, 73 (1993).
- Nasir, M., Matsumoto, H., Minagawa, M., Tanioka, A., Danno, T., Horibe, H., Preparation of porous PVDF nanofiber from PVDF/PVP blend by electrospray deposition. *Polym. J.*, 39, 1060 (2007).
- Omrani, A., Rostami, A. A., Ravari, F., Advanced isoconvensional and master plot analyses on solid-state degradation kinetics of a novel nanocomposite. *J. Therm. Anal. Calorim.*, 111, 677 (2013).
- Osinska, K., Czekaj, D., Thermal behavior of BST/PVDF ceramic-polymer composites. *J. Therm. Anal. Calorim.*, 113, 69 (2013).
- Ozawa, T., Kinetics of non- isothermal crystallization. *Polymer*, 12, 150 (1971).
- Qiu, Z., Mo, Z., Yu, Y., Zhang, H., Sheng, S., Song, C., Non-isothermal melt and cold crystallization kinetics of poly(aryl ether ketone ether ketone ketone). *J. Appl. Polym. Sci.*, 77, 2865 (2000).
- Rajabzadeh, S., Liang, C., Ohmukai, Y., Maruyama, T., Matsuyama, H., Effect of additives on the morphology and properties of poly (vinylidene fluoride) blend hollow fiber membrane prepared by the thermally induced phase separation method. *J. Membr. Sci.*, 423, 189 (2012).
- Sencadas, V., Costa, C. M., Gómez Ribelles, J. L., Lanceros-Mendez, S., Isothermal crystallization kinetics of poly(vinylidene fluoride) in the  $\alpha$ -phase in the scope of the Avrami equation. *J. Mater. Sci.*, 45, 1328 (2010).

- Senum, G. I., Yang, R. T., Rational approximations of the integral of the Arrhenius function. *J. Therm. Anal.*, 11, 445 (1977).
- Song, L. and Qiu, Z., Influence of low multi-walled carbon nanotubes loadings on the crystallization behavior of biodegradable poly(butylenes succinate) nanocomposites. *Polym. Adv. Technol.*, 22, 1642 (2011).
- Supaphol, P., Thanomkiat, P., Phillips, R. A., Influence of molecular characteristics on non-isothermal melt-crystallization kinetics of syndiotactic polypropylene. *Polym. Test.*, 23, 881 (2004).
- Vyazovkin, S., Is the Kissinger equation applicable to the processes that occur on cooling? *Macromol. Rapid. Commun.*, 23, 771 (2002).
- Vyazovkin, S., Wight, C. A., Isothermal and nonisothermal reaction kinetics in solids: In search of ways toward consensus. *J. Phys. Chem.*, 101, 8279 (1997).
- Xiong, H., Gao, Y., Li, H. M., Non-isothermal crystallization kinetics of syndiotactic polystyrene – polystyrene functionalized SWNTs nanocomposites. *eXPRESS Polym. Lett.*, 1, 416 (2007).
- Yu, W., Zhao, Z., Zheng, W., Long, B., Jiang, Q., Li, G., Ji, X., Crystallization behavior of poly(vinylidene fluoride)/montmorillonite nanocomposite. *Polym. Eng. Sci.*, 49, 491 (2009).
- Zhong, G., Zhang, L., Su, R., Wang, K., Fong, H., Zhu, L., Understanding polymorphism formation in electrospun fibers of immiscible poly(vinylidene fluoride) blends. *Polymer*, 52, 2228 (2011).
- Ziabicki, A., Crystallization of polymers in variable external conditions 1. General Equations, *Colloid. Polym. Sci.*, 274, 209 (1996).